2. Dávid Péter Kovács, Ilyes Batatia, Eszter Sára Arany, and Gábor Csányi. Evaluation of the mace force field architecture: From medicinal chemistry to materials science. The Journal of Chemical Physics, 159(4), 2023.
3. Arslan Mazitov, Filippo Bigi, Matthias Kellner, Paolo Pegolo, Davide Tisi, Guillaume Fraux, Sergey Pozdnyakov, Philip Loche, and Michele Ceriotti. Pet-mad, a lightweight universal interatomic potential for advanced materials modeling, 2025.
4. Cesare Malosso, Filippo Bigi, Paolo Pegolo, Joseph W. Abbott, Philip Loche, Mariana Rossi, Michele Ceriotti, and Arslan Mazitov. High-quality, high-information datasets for universal atomistic machine learning, 2026.

Student symposium, session III, May 26, Tuesday

SL9

CRYSTAL STRUCTURE VALIDATION WITH THE USE OF THE DFT METHOD

F. Fňukal

University of Chemistry and Technology, Prague, Technická 5, 166 28 Praha 6 – Dejvice
fnukalf@vscht.cz

Introduction

Current crystal structure validation procedures rely primarily on diffraction data analysis, as implemented in tools such as PLATON/checkCIF [1]. A complementary approach – comparison of the geometry of experimental structures with their DFT-optimized geometries – was introduced by van de Streek & Neumann [2, 3], but did not gain widespread adoption due to high computational demands and reliance on commercial software. Recent advances in computing power and DFT methodology now make this approach practically viable for routine use on standard desktop hardware even for organic molecular crystals with large unit cells.

Method

To facilitate practical application of this approach, we implemented the validation workflow in the program checkCIF-DFT, a freely available program that automates parsing CIF files, management of DFT geometry optimizations via the use of external DFT programs and evaluation of structural discrepancies using a set of comparison descriptors. In our testing so far, geometry optimizations were performed using CASTEP [4] with the r2SCAN [5] meta-GGA functional and Many-Body Dispersion (MBD) correction [6]. Our descriptor set extends the previously proposed r.m.s. Cartesian displacement (RMSCD) [2, 3] with maximum changes in bond lengths, bond angles and torsion angles, maximum Cartesian displacement and a temperature-corrected volume difference – the latter accounting for the formal 0 K conditions of DFT optimization using thermal expansion coefficients derived from Cambridge Structural Database (CSD) [7] data [8].

Results

To set reference values of comparison descriptors, the method was benchmarked against two reference sets: five structures determined by neutron diffraction, representing correct high-quality experimental determinations, and five incorrect structures known to be obtained by data manipulation and fraud [9]. The use of our extended comparison descriptor set is justified as the use of the original RMSCD criterion fails to flag three of the five fraudulent structures as problematic, which was already noted by van de Streek & Neumann in their work. However, the extended comparison descriptor set – particularly maximum bond length difference and maximum bond angle difference – clearly separated all five fraudulent structures from the neutron structures supporting the idea of the need for a multi-parameter validation approach.

The validation procedure was next applied to a representative set of 100 organic crystal structures drawn from the CSD. Of these, 90 calculations completed and the large majority showed deviations consistent with correct experimental determinations (see Fig. 1). However, a subset showed elevated deviations revealing several recurring categories of structural problems: unmodelled solvent-accessible voids, missing atoms, incorrect space group assignment etc. Notably, several calculation failures were also associated with structures showing some of these problems, which offers a possible explanation to the calculation difficulties.

Conclusions

Our results suggest that DFT-based crystal structure validation may serve as a physically grounded complementary validation method to conventional validation checks. This independent validation is of great use especially in cases where determination errors were made but are difficult to spot or in cases where determination details are poorly documented. Furthermore, the results suggest that the CSD is not free of structures with serious structural issues, even among those that have passed conventional validation filters. Our implementation of the method – the program checkCIF-DFT – is planned to be made freely available and is intended to make this DFT validation workflow accessible to the broad crystallographic community. Additionally, it is planned to extend checkCIF-DFT with pre-calculation checks to reveal most common structural issues that are identifiable prior to DFT optimization calculations. Furthermore, support for the use of Machine Learning Interatomic Potentials (MLIPs) is being developed as a significantly faster alternative to DFT calculations.

1. A. L. Spek, Acta Cryst., D65, (2009), 148.

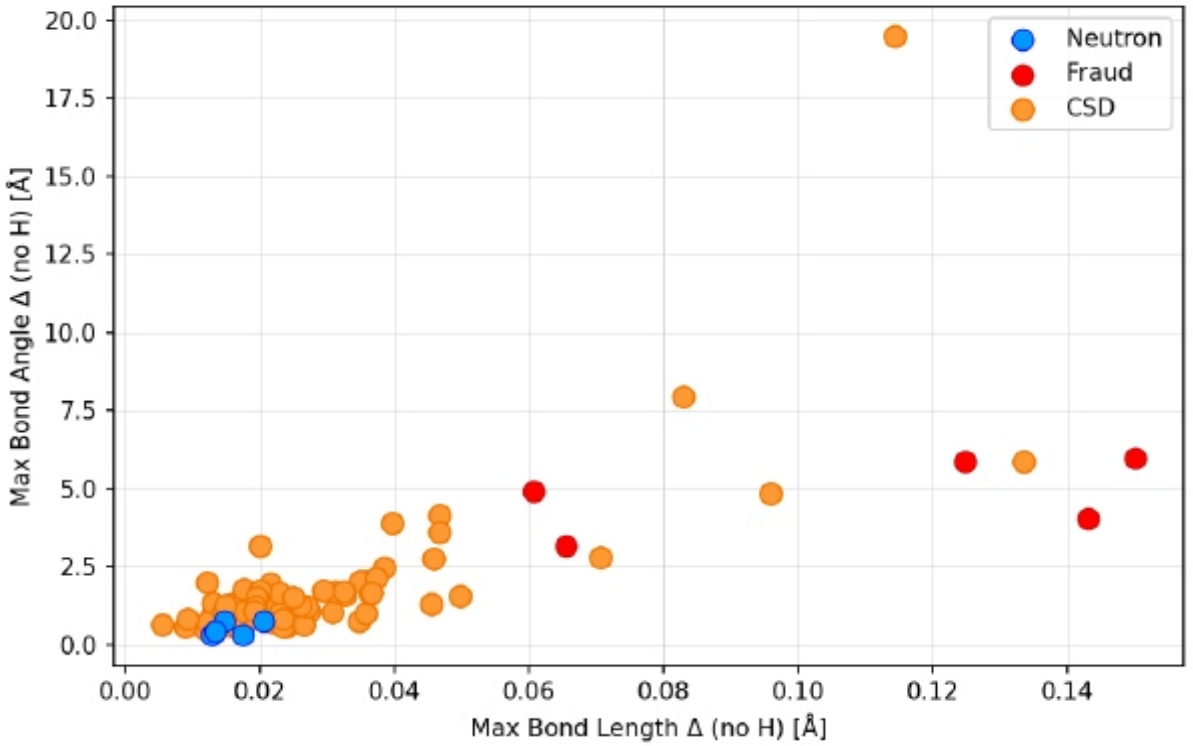

Figure 1. Maximum bond length difference versus maximum bond angle difference for the neutron structures (blue circles), fraudulent structures (red circles) and 90 successfully calculated CSD structures (orange circles) calculated excluding hydrogen atoms.

2. J. van de Streek, M. A. Neumann, Acta. Cryst., B66, (2010), 544.
3. J. van de Streek, M. A. Neumann, Acta Cryst., B70, (2014), 1020.
4. S. J. Clark, M. D. Segall, C. J. Pickard, P. J. Hasnip, M. I. J. Probert, K. Refson, M. C. Payne, Z. Kristallogr., 220, (2005), 567.
5. J. W. Furness, A. D. Kaplan, J. Ning, J. P. Perdew, J. Sun, J. Phys. Chem. Lett., 11, (2020), 8208.
6. A. Tkatchenko, R. A. DiStasio Jr., R. Car, M. Scheffler, Phys. Rev. Lett., 108, (2012), 236402.
7. A. van der Lee, D. G. Dumitrescu, Chem. Sci., 12, (2021), 8537.
8. F. H. Allen, Acta Cryst., B58, (2002), 380.
9. W. T. Harrison, J. Simpson, M. Weil, Acta Cryst., E66, (2009), e1.

Computational resources were provided by the e-INFRA CZ project (ID:90254), supported by the Ministry of Education, Youth and Sports of the Czech Republic.

SL10

INTRAMOLECULAR INTERACTIONS IN FERROCENE PHOSPHINOSTIBINES FROM THE PERSPECTIVE OF STRUCTURAL ANALYSIS AND COMPUTATIONAL METHODS

D. Rezazgui, J. Schulz, P. Štěpnička

Charles University, Faculty of Science, Hlavova 8, 128 00, Praha 2, Czech Republic

This contribution examines intramolecular non-covalent interactions in ferrocene phosphinostibines from the perspective of X-ray structural analysis and computational methods. Hybrid ligands combining phosphine and stibine donor groups were prepared in both flexible and rigid ferrocenyl frameworks, including 1,2-disubstituted phosphinostibines, their phosphine chalcogenides, gold complexes, and the corresponding oxidized stiboranes.

The primary focus is placed on intramolecular donor-acceptor interactions studied via single-crystal X-ray diffraction and theoretical calculations. The diffraction data reveal a clear dependence of the intramolecular contacts on the electronic state of the antimony center. Whereas neutral phosphinostibines show only limited evidence for attractive donor-acceptor interaction, oxidation to stiboranes generates significantly shortened P···Sb, Au···Sb and E···Sb contacts (E = O, S, Se), indicating pronounced pnictogen-centered Lewis acidity and effective intramolecular donor stabilization. In the rigid 1,2-disubstituted ferrocene series, these effects are particularly well resolved, allowing direct comparison of the structural consequences of donor type, oxidation state, and geometric preorganization. The shortest and most distinct interactions are observed for oxygen donors, while the sulfide and selenide analogues exhibit weaker but still recognizable trends.

The nature of these non-covalent interactions was further investigated using Density Functional Theory (DFT) and Intrinsic Bond Orbital (IBO) analysis together with Atoms In Molecules (AIM) analysis. The calculations confirmed the presence of pnictogen bond which upon oxidation of the stibine moiety to stiborane changed into covalent interaction [1-3].

The synergy between X-ray diffraction and quantum chemical modeling thus enables the rational design of new ligands, where these secondary interactions can be utilized to fine-tune reactivity.

1. D. Rezazgui, J. Schulz, P. Štěpnička, *Chem. Commun.* 61 (2025) 18705-18708.
2. D. Rezazgui, J. Schulz, P. Štěpnička, *Inorg. Chem.* 64 (2025) 11075-11092.
3. J. Schulz, J. Antala, D. Rezazgui, I. Císařová, P. Štěpnička, *Inorg. Chem.* 62 (2023) 14028-14043.

This work was supported by the Czech Science Foundation (project no. 21-02316S) and Charles University Research Centre program (project no. UNCE/24/SCI/010). Computational resources were provided by the e-INFRA CZ project (ID: 90254), supported by the Ministry of Education, Youth and Sports of the Czech Republic.

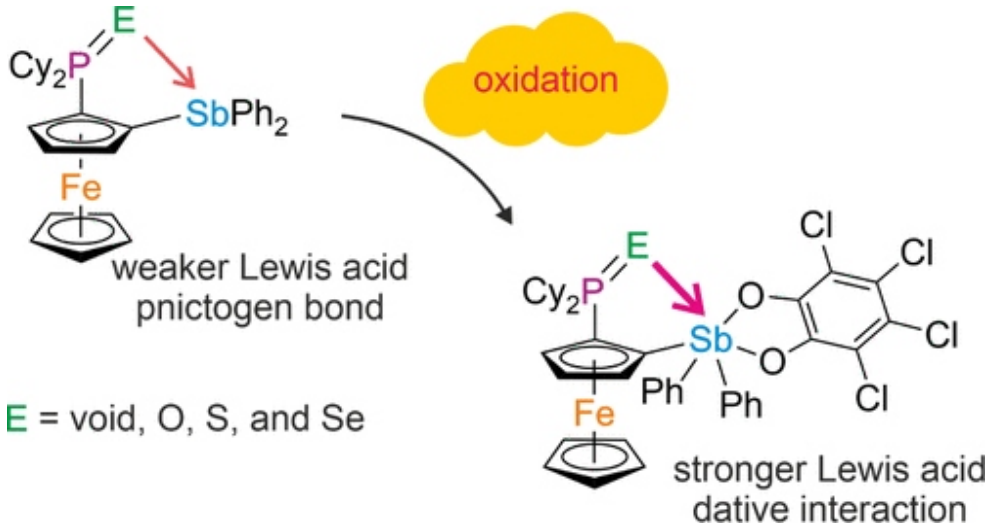

SL11

HOST–GUEST INTERACTIONS IN MIL-140C: COMPUTATIONAL AND EXPERIMENTAL STUDY WITH FOCUS ON PARACETAMOL ENCAPSULATION

Javier García[1], Miroslav Pospíšil[1], Jan Demel[2], Matouš Kloda[2]

[1]*Charles University, Ke Karlovu 3,12116 Prague 2*
[2]*Institute of Inorganic Chemistry, CAS, Husinec-Řež č. p. 1001*
joregjgarciaj@outlook.com

Metal–organic frameworks (MOFs) of the MIL-140 series (A, B, C, D) combine high structure stability with one-dimensional channels with a diameter of ~10 Å, making them very attractive for drug delivery. In this work we present a combined computational and experimental study on paracetamol encapsulation in MIL-140C. Computational pre-screening of nine common drugs was built in Materials Studio (Forcite module, Universal force field (UFF), rigid framework). Paracetamol was ranked as the most affine guest, exhibiting the lowest total potential energy (–223.26 kcal/mol) for two molecules per cell, (Tab. 1). A testing of concentration series for paracetamol (2–8 molecules per cell), (Tab. 2), predicted an optimal loading of four molecules, (Fig. 1), which reached the total minimum potential energy (–237.70 kcal/mol) and showed favourable head-to-tail hydrogen bonding with the framework.

Based on these calculation predictions, MIL-140C was synthesised and the best crystalline sample was selected for adsorption tests with paracetamol and different solvents. Simulated powder X-ray diffraction (PXRD) patterns of the loaded MOF (four paracetamol per cell) show subtle peak shifts and intensity variations compared to the empty framework (Fig. 2), (experimental data pending) consistent with pore occupation. Experimental BET measurements of the paracetamol-loaded sample gave a reduction of surface area (Tab. 3). This decrease, together with the absence of crystalline paracetamol peaks in experimental PXRD (data pending), strongly suggests encapsulation of paracetamol molecules rather than mere surface adsorption.

We explicitly discuss the limitations of our simulations (rigid framework, (UFF), no solvent, idealised crystalline structure) and argue that while computational screening is valuable for ranking affinities, quantitative predictions require more advanced methods. Our integrated approach demonstrates that MIL-140C is a viable platform for paracetamol delivery. Four-molecules of paracetamol were the most efficient loading. These calculation models can

Table 1. Energy comparison of nine pairs of guest molecules tested on MIL-140C

Guest Molecule	Total potential energy [kcal/mol]
Paracetamol	-223.26
Ibuprofen	-3.30
Atenolol	16.04
Bisphenol A	17.19
Diclofenac	21.04
Carbomazepine	56.61
3-Hydroxycarbamazepine	61.10
Caffeine anhydrous	92.34
Sulfamethoxasol	219.15

Table 2. Energy comparison of different amounts of paracetamol

# of Paracetamol	Total binding energy [kcal/mol]	Binding energy per paracetamol [kcal/mol]
2	-90.76	-45.38
3	-115.26	-38.42
4	-237.70	-59.43
5	-45.17	-9.03
6	-41.36	-6.90
7	-40.71	-5.81
8	-2.41	-0.30

Table 3. Experimental BET surface areas (N2 adsorption, 77 K) of MIL-140C with different solvents

Sample	Solvent	BET [m^2 /g]	Change vs. pure MOF
MIL-140C (pure)	----	862.8	----
MIL-140C + paracetamol	2-Propanol	774.4	-10.2 %
MIL-140C + paracetamol	Tetrahydrofuran	789.7	-8.5 %
MIL-140C + paracetamol	Ethyl acetate	762.8	-11.6 %
MIL-140C + paracetamol	Chloroform	74.8	-91.3 %

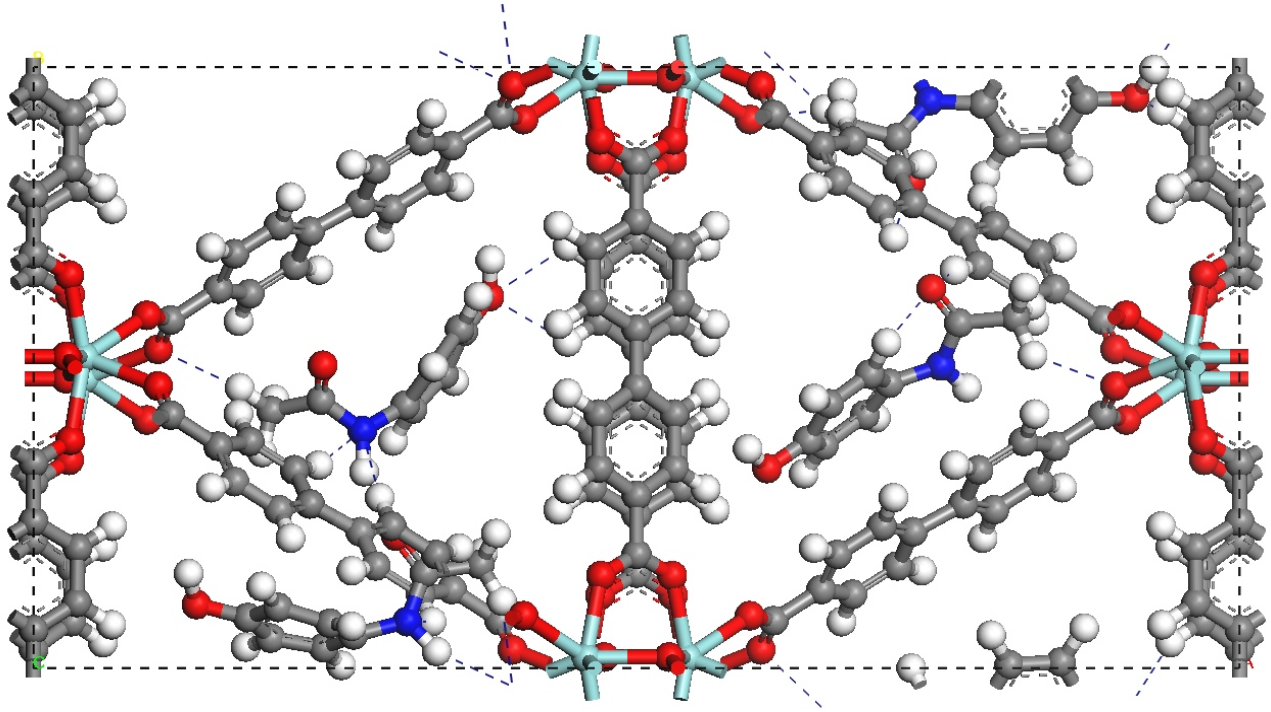

Figure 1. Most stable position of four molecules of paracetamol per unit cell of MIL-140C, after quench dynamics (Forcite, UFF). The blue scattered lines represent hydrogen bonds.

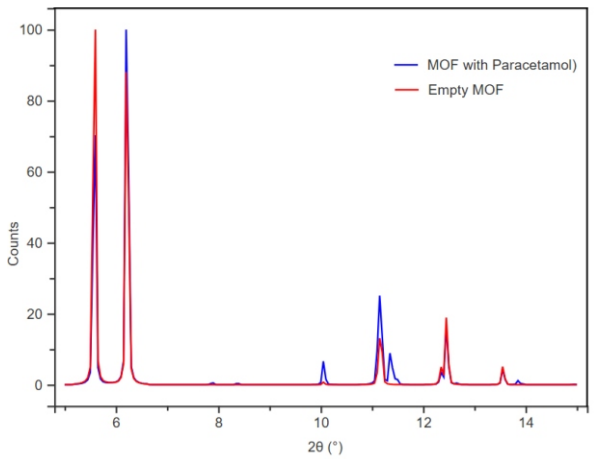

Figure 2. Comparison of simulated Powder X-Rays diffraction of the empty MOF (RED), MOF filled with 4 paracetamols (BLUE).

serve as the first step of prediction of host-guest interaction of various drugs, which will be subsequently tested in *in-vitro* studies.

1. D. Bell, "The Promise of Metal–Organic Frameworks for Use in Liquid Chromatography." LCGC North America, 36(6), (2018).
2. S. A. E. Naser, K. O. Badmus, and L. Khotseng, "Synthesis, Properties, and Applications of Metal Organic Frameworks Supported on Graphene Oxide." *Coatings*, **13**(8), (2023), 1456.
3. Y. Inokuma, S. Yoshioka, J. Ariyoshi, et al., "X-ray analysis on the nanogram to microgram scale using porous complexes." *Nature*, **495**, (2013), 461-466.
4. R. A. Granberg and Ĺ. C. Rasmuson, "Solubility of paracetamol in pure solvents." *Journal of Chemical and Engineering Data*, **44**(6), (1999), 1391-1395.
5. W. Liang, R. Babarao, T. Church, and D. M. D'Alessandro, "Tuning the cavities of zirconium-based MIL-140 frameworks to modulate CO2 adsorption." *Chemical Communications*, **51**, (2015), 11286.
6. V. Guillem, F. Ragon, M. Dan-Hardi, T. Devic, M. Vishnuvarthan, B. Campo, A. Vimont, G. Clet, Q. Yang, G. Maurin, G. Férey, A. Vittadini, S. Gross, and C. Serre, "A Series of Isoreticular, Highly Stable, Porous Zirconium Oxide Based Metal–Organic Frameworks." *Angewandte Chemie International Edition*, **51**, (2012), 9267-9271.
7. L. Samperisci, A. Jaworski, G. Kaur, K. P. Lillerud, X. Zou, and Z. Huang, "Probing Molecular Motions in Metal–Organic Frameworks by Three-Dimensional Electron Diffraction" *Journal of the American Chemical Society*, **143**(43), (2021), 17947-17952.
8. S. Dwivedi, M. Kowalik, N. Rosenbach, D. S. Alqarni, Y. K. Shin, Y. Yang, J. C. Mauro, A. Tanksale, A. L. Chaffee, and A. C. T. van Duin, "Atomistic Mechanisms of Thermal Transformation in a Zr-Metal Organic Framework, MIL-140C." *The Journal of Physical Chemistry Letters*, **12**(1), (2021), 177-184.